Journal of Biomedical Materials Research Part A

Low density polyethylene functionalized with antibiofilm compounds inhibits Escherichia coli cell adhesion

Journal:	*Journal of Biomedical Materials Research: Part A*
Manuscript ID	JBMR-A-17-0292.R1
Wiley - Manuscript type:	Original Article
Date Submitted by the Author:	n/a
Complete List of Authors:	Dell'Orto, Silvia; University of Milan, Pharmaceutical Sciences Cattò, Cristina; University of Milan, Department of Food, Environmental and Nutritional Sciences Villa, Federica; University of Milan, Department of Food, Environmental and Nutritional Sciences Forlani, Fabio; University of Milan, Department of Food, Environmental and Nutritional Sciences Vassallo, Espedito; CNR, Istituto di Fisica del Plasma CNR Morra, Marco; Nobil Bio Ricerche S.p.A., Lab Cappitelli, Francesca; University of Milan, Department of Food, Environmental and Nutritional Sciences Villa, Stefania; University of Milan, Pharmaceutical Sciences Gelain, Arianna; University of Milan, Pharmaceutical Sciences
Keywords:	Low density polyethylene, coupons, antibiofilm activity, p-aminocinnamic acid,p-aminosalicylic acid.

Low density polyethylene functionalized with antibiofilm compounds inhibits *Escherichia coli* cell adhesion

Silvia Dell'Orto[1], Cristina Cattò[2], Federica Villa[2], Fabio Forlani[2], Espedito Vassallo[3], Marco Morra[4], Francesca Cappitelli[2], Stefania Villa[1]*, Arianna Gelain[1]

[1]Department of Pharmaceutical Sciences, Università degli Studi di Milano, Via L. Mangiagalli 25, 20133 Milano, Italy.
E-mail: stefania.villa@unimi.it.
[2]Department of Food Environmental and Nutritional Sciences, Università degli Studi di Milano, Via Celoria 2, 20133 Milan, Italy.
[3]Institute of Plasma Physics «Piero Caldirola», National Research Council (CNR), Via Roberto Cozzi, 53 20125 Milan, Italy.
[4]Nobil Bio Ricerche S.r.l, Via Valcastellana 28, 14037 Portacomaro (AT), Italy

Abstract.

The present work concerns an efficient strategy to obtain novel medical devices materials able to inhibit biofilm formation. The new materials were achieved by covalent grafting of *p*-aminocinnamic or *p*-aminosalicylic acids on low density polyethylene coupons. The polyethylene surface, previously activated by oxygen plasma treatment, was functionalized using 2-hydroxymethylmetacrylate as linker. The latter was reacted with succinic anhydride affording the carboxylic end useful for the immobilization of the antibiofilm molecules. The modified surface was characterized by Scanning Electron Microscope, X-ray photoelectron spectroscopy, attenuated total reflectance Fourier transform infrared and fluorescence analyses. The antibiofilm activity of the modified materials were tested against *Escherichia coli* biofilm grown in the Center of Disease Control biofilm reactor. The results revealed that the grafted cinnamic and salicylic acid derivatives reduced biofilm biomass, in comparison with the control, by 73.7±10.7% and 63.4±7.1% respectively.

Keywords:

Low density polyethylene, coupons, antibiofilm activity, *p*-aminocinnamic acid, *p*-aminosalicylic acid.

Introduction

With advancements in materials science over the past few decades, it has been observed a dramatic increase in the use of synthetic polymers in our everyday life. Polymeric materials are widely used in industrial and engineering applications, as well as in clinical settings.

Synthetic polymers, as any other surface, do not escape from being colonized by microorganisms in form of biofilms, a complex microbial community embedded in a self-produced extracellular polymeric matrix[1,2] Within the biofilm matrix, microorganisms undergo processes of cell specialization, enabling coordinated and efficient survival strategies

against external attacks.[3,4] Once the biofilm is established on the surface, it can damage the structure and function of polymeric materials and it can act as a source of infections for humans, animals and plants[5] The most detrimental property of biofilms is the remarkable resistance to traditional antimicrobial agents (up to 1000-fold in comparison to their planktonic counterpart), which makes biofilm eradication one of the most important societal and economic challenge of the modern era.[6,7]

It seems clear that the best approach to eradicate biofilms is to prevent their formation. To date, strategies employed to prevent unwanted biofilms on both medical and industrial polymers mainly consist of: (a) spreading a broad-spectrum antimicrobial agent on the material surface;[8,9] (b) mixing in bulk material polymers with antibacterial agents and their copolymerization[10,11] (c) surface modification to control the physicochemical interactions between the microorganism and the polymeric surface.[12] Coating polymers with bioactive agents or entrapping them into the materials are the simplest approaches to obtain products with anti-biofilm properties.[13] These strategies are primarily based on the use of traditional antimicrobial agents, widely applied in both clinical and industrial settings.

Although the idea to combine materials in use with antimicrobial substances appears straightforward, low drug release from bioactive materials, that can not be monitored or quantified, contributes to the serious phenomenon of multidrug resistance spreading,[14] making this approach less attractive for a subsequent application. In addition, the non-uniform distribution of substances inside the material, and the formation of aggregates due to the incomplete miscibility, make these polymers undesirable materials in many applications.[10]

Therefore, new approaches become imperative, and a serious change in our prospective is necessary: instead of fighting biofilm with antimicrobial materials and coatings, the efforts should be directed towards developing innovative anti-biofilm materials with functional features targeting molecular determinants of biofilm genesis (e.g. substratum adherence),

disarming microorganisms without killing them.[15,16] Active substances with well-known anti-biofilm activity at low concentrations would not be leached from the surface, avoiding the problem of the compound kinetics release, and providing long-term protection against microbial colonization. Depriving microorganisms of their biofilm-specific traits, without affecting their existence, may also decrease selection pressure for drug-resistant mutations, restoring the efficacy of the current arsenal of antimicrobial agents. In fact, this strategy does not presume to be the only solution to prevent biofilm development, but rather it should be used in combination with other treatments to maximize the anti-biofilm performances of the new polymeric materials.

An example of biocide-free anti-biofilm compounds is offered by the secondary metabolite of the seagrass *Zostera marina*, the zosteric acid. It was previously demonstrated that zosteric acid possesses the remarkable ability to counteract microbial adhesion and subsequent biofilm formation, to shape fungal biofilm architecture, to potentiate the performance of conventional antimicrobial agents and to show cytocompatibility towards soft and hard mammalian tissue cell based models.[17-19] In the past years, few attempts have been made to incorporate zosteric acid into silicone coatings in order to achieve its slow release in the surrounding area.[10,20] However, to the best of our knowledge, nobody investigated the possibility to design a non-leaching, long lasting, anti-biofilm material to prevent colonization of polymeric materials, by using biocide-free compounds able to hinder biofilm formation. In our previous study,[16] we designed and screened against *Escherichia coli* a 43-member library of small molecules based on zosteric acid scaffold diversity to understand the structural requirements necessary for biofilm inhibition, and to identify functional groups that could be exploited for the covalent linkage to an abiotic surface. This work revealed that *p*-aminocinnamic acid, targeting WrbA a FMN-dependent oxido-reductase,[16] is able to significantly reduce *E. coli* biofilm formation, and it could be considered as an excellent candidate to be covalently linked to a polymeric

support due to the presence of an amine at the *para* position on the phenyl ring. Besides cinnamic acid analogues, another class of derivatives related to the scaffold of salicylic acid has been investigated. To date, salicylates are known to be powerful antimicrobial agents against a wide range of fungi and bacteria[21] and they are able to prevent bacterial adhesion on medical devices.[22] Their biological investigation led us to the identification of the commercially available *p*-aminosalicylic acid as a suitable antibiofilm compound used as reference in the grafting process. Moreover, among the proteins targeted by salicylic acid (WrbA, MenI), we have recently identified a tryptophanase involved in indole synthesis, TnaA.[23] This paper is focused on the functionalization of a polymeric support with *p*-aminocinnamic acid and *p*-aminosalicylic acid in order to obtain novel materials able to hinder *E. coli* biofilm formation. In contrast to a LDPE film, a 1.6 mm thick coupon with a polymeric surface was prepared for the immobilisation of biologically active molecules by a multi-step process. A low-pressure plasma reactor system[24] was used for an efficient activation of the polymeric surfaces, as well as for the grafting-polymerization process. Several analytical techniques performed to characterize each step of the functionalization process are herein described, and the obtained data are reported.

Experimental Section

Material and methods

Low-density polyethylene (LDPE) used in this study was purchased from Alfa Aesar, as sheets (300 x 300 x 1.6 mm). Samples were prepared as 1.6 mm (0.063 inch) thick round shape coupons (d=1.27cm). 2-Hydroxyethyl methacrylate (97 %, containing ≤ 250 ppm monomethyl ether hydroquinone as inhibitor), *p*-aminocinnamic acid and *p*-aminosalicylic acid such as reagents and solvents for surface activation and Luria-Bertani broth were

purchased from Sigma Aldrich and used as received without any further purification. AUSILAB 101, used for coupons cleaning was purchased from Carlo Erba Reagents.

LDPE Activation procedure

Cleaning of LDPE coupons

Polyethylene coupons were washed with a 3 % w/v aqueous solution of a neutral detergent (AUSILAB 101) efficient in removing greasy residues and then with a 1 M HCl. They were subsequently purified by extraction with acetone overnight and dried prior each plasma treatment.

Plasma activation of LDPE

The apparatus used for this study consisted of a parallel-electrodes, capacitive-coupled plasma enhanced chemical vapour deposition (PECVD) system, made up of a cylindrical stainless steel vacuum chamber of 25 cm inner diameter with an asymmetric electrode configuration. The powered electrode was connected to a 13.56 MHz power supply, associated to an automatic impedance matching unit, while the other electrode was grounded and worked as sample holder. The treatment was performed for 60 s at a total plasma process pressure of about 15 Pa, kept constant by balancing the incoming oxygen flux with the system pumping speed. Commercially available oxygen (99.998% purity) was supplied into the discharge vessel through a mass flow controller. The total gas pressure was measured by a capacitive vacuum gauge. Plasma treatment was performed at fixed RF power of 100 W. At first low pressure was created in the process reactor by means of a turbo-molecular pump combined with a rotary pump. At a process pressure of 2.6 Pa, oxygen was fed into the chamber (O_2 flow= 15 sccm).

Coupons of commercial LDPE, previously washed and inserted into the vacuum chamber, were exposed to low pressure oxygen plasma for surface activation. The process parameters were kept constant during the whole activation. Contact angle measurements were used to evaluate the effectiveness of the process. As known, a LDPE treatment with oxygen plasma modifies the wettability of surface. The increase in wettability is due to the presence of varieties of oxygen containing groups on the surface, (such as -C-O, -C=O, -O-C=O, -OH, -OOH, etc.) after plasma treatment.[25] The water contact angle of untreated LDPE was estimated 70°. The contact angle measurement immediately after the plasma process was estimated < 10°. As expected, the wettability (surface energy) was strongly increased. Because of quickly ageing of the treated surface (loss of the wetting properties), the grafting procedure was performed immediately after the extraction of the sample from the process chamber.

The grafting procedure: LDPE-HEMA-OH surface

In the graft-polymerization process, monomers were introduced into the vacuum chamber as a layer on the plasma pre-treated surface. In details, LDPE samples were dipped for 10s in a 0.1 M solution of HEMA in ethanol. Then, the coupons were completely dried in air and oxygen plasma treated in order to promote the graft-polymerization of the monomer. In the latter process, free-radicals are generated on the samples surfaces by the plasma species bombardment (mainly ions), promoting the graft-polymerization of the pre-adsorbed monomers. Input power was kept constant at 100 W as well as the grafting treatment time (60s), in order to prevent damaging of substrates.[26] The samples were finally ultrasonically washed in ethanol for 5 minutes in order to remove the ungrafted molecules and dried in air at room temperature.

Preparation of the LDPE-HEMA-COOH surface

The LDPE-HEMA-COOH film was obtained by treatment of the LDPE-HEMA-OH film with succinic anhydride. In a conical flask the coupons were dipped in 10 mL of dichloromethane, with dry pyridine (2.5 eq). Succinic anhydride (2.5 eq) dissolved in 10 mL of THF was added to the reaction mixture. The suspension was allowed to proceed at room temperature for 24 h. The coupons were washed with copious amounts of dichloromethane (10 x 10 mL) prior to dry in air. Since it was not possible to evaluate exactly the equivalent of hydroxyl groups introduced on polyethylene due to the difficulty of analysis, related to coupons thickness, a general assessment of the number per unit area was made on the basis of literature data.[27]

General procedure to graft selected molecules to the LDPE-HEMA-COOH surface via amide bond formation

The carboxylic groups of LDPE-HEMA-COOH coupons (1 eq) were activated by dipping the surfaces into a dichloromethane solution (10 mL) of N-hydroxysuccinimide (1.2 eq), and N,N-dicyclohexylcarbodiimide (1.2 eq) under a nitrogen atmosphere at room temperature for 20 min. Then the suitable compound (1.2 eq of p-aminocinnamic acid or p-aminosalicylic acid) was poured into the suspension and the resulting mixture was stirred at room temperature for 16 h. Coupons were filtered off and washed with copious amounts of dichloromethane (10 x 5 mL). Additional washes with DMF (3 x 5 mL) were necessary to remove completely the dicyclohexylurea from the surfaces. The coupons were dried in vacuo to allow analytical analysis. Similarly to the LDPE-HEMA-OH coupons, the equivalent of carboxylic groups introduced on the surface was not precisely determined, thus the subsequent grafting was performed using an excess of all reagents to ensure the amide bond formation.

Characterization of the modified LDPE surface

Scanning Electron Microscope (SEM) analysis

Surfaces of the oxygen plasma activated polyethylene coupons were examined with a Leo 1430 scanning electron microscopy (Zeiss, Oberkochen, Germany) to gather data on the overall physical organization of the polymer network.

X-ray Photoelectron Spectroscopy (XPS) analysis.

Measurements were carried out using a Perkin Elmer PHI 5400 ESCA System equipped with a monochromatic X-ray source (Mg Ka anode) operating at 10 kV and 200 W. Analyzed volume was given by the diameter of the photon beam at the sample surface (5 mm) and by the depth of analysis of about 8-10 nm. The base pressure was kept at 10-8 Pa. Curve fitting and quantification of elements were accomplished using the software and the sensitivity factors supplied by the manufacturer.

Attenuated total reflectance infrared spectroscopy (ATR-FTIR) analysis.

FTIR measurements were performed using a SpectrumOne spectrophotometer (Perkin-Elmer, USA), by placing the coupons on a diamond crystal mounted in ATR cell (Perkin-Elmer, USA). The spectra were collected over the wavenumber region 4000−650 cm^{-1} at 4 cm^{-1} resolution and 128 scans. The FTIR-ATR measurements provided mostly qualitative information on the chemical changes of the near-surface region. The measured thickness of the layer was limited to 4 μm. Experiments were carried out under ambient conditions.

Fluorescence analyses.

Fluorescence measurements were carried out in a Perkin-Elmer LS 50B spectrofluorometer equipped with PTP-1 Fluorescence Peltier System. Excitation and emission spectra were recorded at 50 nm/min, with both emission and excitation slit widths set at 3.0 nm (20°C) when free molecules in solution (0.2–5.0 mM) were measured. The measurements of coupons

fluorescence spectra were achieved at 100 nm/min, at room temperature, with both emission and excitation slit widths set at 2.5 nm using the front surface accessory.

Confocal Scanning Laser Microscopy

The untreated and functionalized coupons were visualized using a Leica SP5 Confocal Laser Scanning Microscope (CLSM) (405 nm laser excitation line, blue channel). Images were captured with a 40x, 0.8 NA water immersion objective and analysed with the software Imaris (Bitplane Scientific Software, Zurich, Switzerland). In order to assess the stability of the functionalized and non-functionalized materials, coupons were mounted in the Center for Disease Control Bioreactor (CDC reactor, Biosurface Technologies, Bozeman, MT, USA) and the biofilm were consecutively grown for 10 times on their surface as reported in the following section 'Biofilm formation assay'. After each round of biofilm formation, coupons were removed from the CDC reactor, placed in a sonication bath (2 min, 50% amplitude, Branson 3510, Branson Ultrasonic Corporation, Dunburry, USA) to dislodge the biomass and sterilized in 40% ethanol for 1 h[28] The complete removal of biofilm from the coupon surfaces was confirmed by microscope observations. After the tenth growth, coupons were cleaned from the biomass and analysed again by CLSM. The experiments were repeated three times.

Biofilm formation assay

E. coli K-12 MG1655 was used as a model system to study microbial biofilms, being a cosmopolitan bacterium that shares a core set of genes with clinically-relevant serotypes and foodborne pathogenic strains, including genes involved in biofilm formation.[29] Furthermore, it has a number of other important advantages, namely a well-developed literature base, a complete genetic characterization, and amenability to molecular techniques.[30]

The microorganism was stored at –80°C in suspensions containing 20 % glycerol and 2 % peptone, and was routinely grown in Luria-Bertani broth at 37 °C. *E. coli* biofilm was grown

on functionalized and non-functionalized coupons using the CDC reactor (Biosurface Technologies, Bozeman, MT, USA) according to the literature procedure[31]. The adhesion phase was performed in sterile LB medium while the dynamic phase was performed in sterile 10 % LB medium pumped into the reactor at a rate of 8.3 mL/min. After 48 hours of dynamic phase, functionalized and non-functionalized coupons were removed and gently washed with PBS.

Biofilms grown on functionalised and non-functionalised coupons was stained using 1x commercial solution of CellMask plasma membrane orange stain (Molecular Probes-Life Technologies) in sterile PBS to visualize the total biomass. Biofilms were incubated for 30 min in the dark at room temperature and then rinsed with sterile PBS. Coupons without biofilm were also stained with the dyes in order to exclude any false positive signals. Biofilm samples were visualized using a Nikon Eclipse E800 epifluorescent microscope with excitation at 581 nm and emission at 644 nm for the red channel. Images were captured with a 60x, 1.0 NA water immersion objective and analyzed via MetaMorph 7.5 software (Molecular Devices, Sunnyvale, CA, USA). The surface coverage was obtained from ten random images for each sample for at least three coupons for experiment according to the previous literature[32].

Biofilms grown on functionalized and non-functionalized coupon were also subjected to cryosectioning according to literature.[33] Briefly, biofilms grown in the CDC reactor were carefully covered with a layer of Killik (Bio Optica, Italy) and placed on dry ice until completely frozen. Frozen samples were sectioned at -19°C using a Leitz 1720 digital cryostat (Leica, Italy). The 10-µm thick cryosections were mounted on glass slides, stained with 1x commercial solution of CellMask plasma membrane orange stain (Molecular Probes-Life Technologies) and visualised by epifluorescence microscope following the same procedure adopted for the intact biofilms. Biofilm mean thickness was calculated from at least three

cryosections for experiment by the ImageJ 1.50i software (National Institute of Health, USA) according to literature.[34]

Volumes of biofilm cellular component were estimated as previously reported by de Carvalho et al., 2007.[35]

The efficacy of the antibiofilm material was calculated as percentage decrease of the biofilm surface coverage, thickness and cell volume in the functionalized samples respect to the control images.

ANOVA test, via a software run in MATLAB environment (Version 7.0, The MathWorks Inc, Natick, USA), was applied to statistically evaluate any significant differences among the samples. Tukey's honestly significant different test (HSD) was used for pairwise comparison to determine the significance of the data. Statistically significant results were depicted by p-values < 0.05.

Results and Discussion

LDPE coupons surface functionalization

Low density polyethylene (LDPE), which remains among the most commonly-used polymers in many applications, was chosen as material for the grafting procedure. LDPE is characterized by very low wetting properties in aqueous media and high resistance against a wide range of reagents, including diluted and concentrated acids and bases. This latter property is of primary importance since this material underwent to chemical modifications to become suitable to link anti-biofilm compounds. Up to now, the functionalization of material was performed only on polymeric films,[27,36] whose thickness was around few nanometers. Noteworthy in this work 1.6 mm thickness LDPE coupons were used (in literature are reported studies concerning HDPE coupons modifications[37]), although this choice had entailed a complex characterization of the functionalized surface. Since polyethylene does not

possess the required chemical features to allow grafting with the selected anti-biofilm molecules, plasma technology was employed to improve its surface properties, leading to physical and chemical modifications of the first molecular layers without changing the material bulk.[38] The O_2 plasma treatment of LDPE caused the breakdown of several C–H bonds and the generation of activated species (incorporation of hydrophilic functional groups as carbonyl [C=O] and carboxylic [–COOH] groups).[26] The subsequent exposure of the activated surface of LDPE to the air provoked further oxygen incorporation (surface oxidation). Functional groups could be utilized to initiate the surface free-radical polymerization in a mechanism generally termed graft copolymerization as shown in **Figure 1**.

After the activation of the surface, the LDPE samples were immersed in a solution of 2-hydroxyethyl metacrylate (HEMA) in ethanol, dried in air and then O_2 plasma treated in order to promote the graft polymerization of the monomer (LDPE-HEMA-OH). The activation process, as well as the graft-polymerization that occurred on the LDPE, were followed by the characterization of the surface through scanning electron microscopy (SEM) analyses, X-ray photoelectron spectroscopic (XPS) and attenuated total reflection infrared (ATR-IR) spectroscopy (see below). Then the hydroxyl end groups of the grafted HEMA side chains (LDPE-HEMA-OH) were converted into the corresponding carboxylic acid (LDPE-HEMA-COOH). The final step involved the amide bond formation between the modified surface and *p*-aminocinnamic acid (LDPE-CA) or *p*-aminosalicylic acid (LDPE-SA).

Surface analyses

Scanning Electron Microscope (SEM) analysis

The morphology modification of the samples prepared after activation with oxygen plasma was evaluated by low-vacuum-SEM analysis. The clearly visible surface morphology changes

obtained after plasma treatments were evident from SEM images (**Figure 2**). The topology and the roughness of the originally smoothed surfaces were dramatically changed. In particular, considerable modifications of the surface roughness were detected in the oxygen-plasma-treated samples activated. Indeed, the plasma reactor treatment produced a noticeable increase of roughness resulting in polyethylene characterized by small holes that covered uniformly all the surface. Moreover, same structures were visible also in different parts of the studied sample surfaces reflecting high reproducibility and homogeneity of the applied plasma treatment.

X-ray Photoelectron Spectroscopy (XPS) analysis

The most common technique used to characterize polymeric surfaces is the X-ray photoelectron spectroscopy (XPS). In general, this technique allows the identification of chemical groups on materials and their quantification. In this study, C, O and N at the surface of treated samples were detected using the XPS spectroscopy. The qualitative information resulted from the analysis of the oxidized LDPE surface after plasma treatment, which contained at least carbon and oxygen, and of the functionalized surface composed of an undefined amount of carbon, nitrogen and oxygen. Normally, the XPS analysis of activated polyethylene yielded surface concentration values of 70-80 % carbon, 10-20 % oxygen and trace of nitrogen. The surface compositions detected by XPS analysis were respectively for :

- plasma activated LDPE coupons not functionalized: 16.9 % of oxygen, nitrogen was not detected, 76.4 % of carbon, 6.7 % of silicon and aluminium (**Figure 3** Panel a);

- LDPE coupons functionalized with *p*-aminocinnamic acid (LDPE-CA): 17.9 % of oxygen, 2.7 % of nitrogen, 75.9 % of carbon and 3.5 % of silicon and aluminium (**Figure 3** Panel b);

- LDPE coupons functionalized for instance with *p*-aminosalicylic acid (LDPE-SA): 20.7 % of oxigen, 4.1 % of nitrogen, 75.2 % of carbon and trace of silicon and aluminium. (**Figure 3** Panel c).

An increase of the nitrogen content after the coupling was observed from XPS analysis of functionalized LDPE (LDPE-CA and LDPE-SA). It should be noted that the oxidized layer could be, and in general is, non-homogenous in the vertical direction, with a decreasing concentration of oxygen in relation with an increased depth. However, the error introduced by the assumption of a non-homogeneous distribution of carbon and oxygen is negligible.

According to the obtained data, some observations could be drawn:

- the surface composition of plasma activated polyethylene coupons (**Figure 3** Panel A) was in agreement with the results expected for a polyolefin which underwent oxygen plasma treatment. The signal concentration value of oxygen peak (O1s, ~17 %) indicates a remarkable introduction of oxygen functionalities on the surface, as confirmed from the detailed analysis of carbon peak (C1s, ~77 %).

- XPS spectra of LDPE-CA and LDPE-SA coupons (**Figure 3**, Panel B and C respectively) showed a well-defined nitrogen peak (N1s, ~3 % and 4.1% respectively) in addition to the others peaks detected for not-functionalized coupons. The analysis of N1s peaks revealed that the binding energy of the main components was closed to 400 eV. These results indicated that the nitrogen was not oxidized (absence of nitrite or nitrate groups). The evaluated concentrations were less than the theoretical ones, but it was worth reminding that the depth of the analyzed samples is crucial since the thickness of the monolayer composed by the antibiofilm compounds bound to the linker, was less than 1 nm, while the XPS analysis evaluates the composition of a layer thick around few nanometers, in particular about 8-10 nm in the case of polymers. Therefore, the contribution of signal is almost completely due to the

polymer rather than to the chemical agents although the signal did not decay linearly from the outside to the internal layers and the major contribution was due to the external layers.

- in the samples, some elements (Si, Al) were detected at low concentrations (≤ 7 %), most likely due to some contaminants left on the samples upon the processing techniques. It was very difficult to perform reliable estimation on the surface coverage with the selected molecules. The evaluation of quantitative parameters able to provide indications on the reaction yield in terms of surface functionalization per unit was not easy and required assumptions that were difficult to define. However, the composition data indicated that the immobilization of *p*-aminocinnamic acid led to an increase of O/C ratio and obviously of N/C ratio (as expected from the compounds elemental composition) suggesting a good yield.

Attenuated total reflectance infrared spectroscopy (ATR-FTIR) analysis

In order to detect the presence of the antibiofilm compounds grafted on the polymeric surface, ATR infrared spectroscopy analyses were carried out, considering that plasma surface modifications are confined only to few nanometers below the surface.

ATR-FTIR analysis is one of the main methods used to obtain finer surface information. This technique was used to characterize the polymer surface and the spectra of the treated and the untreated samples were compared to observe the changes. The spectrum of the untreated LDPE is typical of polyethylene with a small number of characteristic peaks.

After plasma exposure of the original material, the characteristic functional groups containing oxygen were introduced and therefore significant variations in the performed spectrum should have been observed. These changes should have been caused by the incorporation of some hydroxy or peroxy groups after the plasma treatment of LDPE with the appearance of two

broad peaks between 3.600–3.050 cm^{-1} and 1.800–1.520 cm^{-1} respectively, since carbonyl stretching is one of the easiest absorptions to recognize in an infrared spectrum and it usually has a very intense band. Despite, according to the recorded spectra, no -OH or -OOH signals were seen in plasma activated samples (see **Figure 4a**) probably due to the low concentration of the polar species on the surface, as well as no changes were observed for LDPE-HEMA-OH grafting and its subsequent oxidation to obtain a carboxylic acid. Noteworthy, after the covalent linkage with *p*-aminocinnamic acid and *p*-aminosalicylic acid the shapes of the spectra changed, as shown in **Figure 4b and c** respectively. These changes are significant especially in the infrared-region between 1.600-1.800 cm-1 (C-O stretching, N-H bending), suggesting that the treated samples spectra are characterized by the typical peaks of the amide bond and confirming the presence of a covalent bond between the antibiofilm molecules and the supporting material.

Fluorescence analyses of the functionalized polyethylene

Fluorescence analyses were performed in order to investigate the polyethylene functionalization with *p*-aminosalicylic acid and *p*-aminocinnamic acid. These molecules are characterized by an intense intrinsic fluorescence (**Figure 5a** and **b**) when they are free in solution, showing emission maxima at 395 nm and 443 nm for *p*-aminosalicylic acid (λ_{exc} = 325 nm) and *p*-aminocinnamic acid (λ_{exc} = 380 nm), respectively.[16] This property allowed us to evaluate the fluorescence of the solid surface of the functionalized polyethylene.

Though the scattering noise typical of these measurements was high, and considering that only a minimal part of the polyethylene coupons (the surface layer) was involved in the functionalization reaction, a difference in the shape of fluorescence spectra of LDPE-SA and LDPE-CA coupons respect to the untreated coupons (LDPE-HEMA-COOH) was observed in the wavelength interval 420-500 nm. The possible specific fluorescence contribute of LDPE-

SA and LDPE-CA was measured by subtracting their solid surface fluorescence spectra with those of the LDPE-HEMA-COOH coupons. A positive fluorescence signal (**Figure 5c** and **d**) was evidenced for both polyethylene materials. The measured emission maxima of the solid surface fluorescence of LDPE-SA and LDPE-CA were 442 nm (λ_{exc} = 334 nm) and 448 nm (λ_{exc} = 385 nm) respectively. Taking into account the different conditions used for the measurement of fluorescence (solid surface *vs.* solution), the features of the LDPE-CA fluorescence are similar to those determined for free *p*-aminocinnamic. In the case of the LDPE-SA the fluorescence features are less similar to those of free *p*-aminosalicylic acid and it is presumably due to the dominance of an intramolecular hydrogen bonded form of *p*-aminosalicylic acid, giving rise to an ultrafast excited state intramolecular proton transfer from the hydroxyl to the carboxyl group.[39] Altogether fluorescence data supported the occurrence of *p*-aminosalicylic acid and *p*-aminocinnamic moieties on the functionalized polyethylene.

Confocal Scannig Laser Microscopy

The fluorescence of *p*-aminocinnamic acid and *p*-aminosalicylic acid immobilized scaffold was also used to verify the surface functionalization by CLSM. Acquired pictures of LDPE, LDPE-HEMA-OH, LDPE-HEMA-COOH and LDPE-HEMA-COOH-DCC (**Figure 6a**) control samples revealed a completely black background with absence of fluorescence. On the contrary, acquired images of LDPE-CA and LDPE-SA samples revealed the presence of an intense fluorescence signal that, since no fluorescence was detected in the control samples, could be attributable to the cinnamic acid and salicylic acid moieties, immobilized on the surface, demonstrating the successful of the functionalization process (**Figure 6b** and **c**).

To prove the retention and the stability of the functionalized materials, the CSLM analysis was repeated on coupons after growing *E. coli* biofilm on their surface for 10 consecutively

times during a period of six months by the CDC reactor. Images from control coupons revealed a completely black background with the absence of fluorescence. Pictures of LDPE-CA and LDPE-SA 10-fold used coupons still revealed the presence of an intense fluorescence signal comparable to that obtained from the corresponding not-used, confirming that coupons were not altered after several washing steps, and that cinnamic and salicylic acids derivatives were successfully retained by the surface (**Figure 6d** and **e**). This data supported the functional stability of LDPE-CA and LDPE-SA coupons, and their long service life.

Antibiofilm evaluation

In order to evaluate the antibiofilm properties of the modified material and to verify the effect of the grafting, the new surfaces were tested by using an *in vitro* system mimicking hydrodynamic flow conditions normally encountered *in vivo.* The CDC biofilm reactor was used to reproduce *E. coli* biofilms at the solid-liquid interface under continuous fluid shear stress. Epifluorescence microscope was used to provide images of biofilm formation.

Direct microscopic visualization of the total biofilm biomass on functionalized and non-functionalized coupons is shown in **Figure 7a-f**, where *in situ* biofilms have been stained with the CellMask plasma membrane orange stain.

Pictures analysis showed significant differences in the percentage of biofilm surface coverage, thickness and biovolume between the control LDPE and the functionalized LDPE-CA and LDPE-SA materials (**Figure 7g**). Indeed, the analysis of the images revealed that LDPE-CA and LDPE-SA functionalized materials reduced biofilm surface coverage by 73.7±10.7 % and 63.4±7.1 % respectively, compared to the control LDPE (**Figure 7g**). Obtained data also showed that biofilm thickness was lower on functionalized surfaces that on the control one. Indeed, a reduction of 84.7±22.1 % and 75.2±14.5 % was observed respectively on LDPE-CA

and LDPE-ZA (**Figure 7g**). Moreover, biovolume resulted in a decrease of 96.0±29.1 % when grown on LDPE-CA and of 90.9±20.4 % on LDPE-SA (**Figure 7g**).

No significant differences were detected in the bacterial surface coverage, biofilm thickness and biovolume between the LDPE control sample and the LDPE-HEMA-OH and LDPE-HEMA-COOH control samples, confirming that the used linker does not affect biofilm formation (**Figure 7a,d,g**).

Coupons without biofilm and stained with the same dye did not produce detectable fluorescence suggesting that false positive signals were not produced (data not shown).

Obtained results are in line with previous data obtained with ZA and SA free in solution, suggesting that the molecules exert their anti-biofilm activity even when immobilized on a surface.[17,19,40-42] It is likely that both immobilized molecules may exploit their anti-biofilm activity with a mode of action similar to that they have free in solution. It has been found that ZA targets key step involved in *E. coli* biofilm formation by modulating the threshold level of the autoinducer-2 signal and inducing a hypermotile phenotype unable to firmly adhere on surfaces.[43] On the other hand, SA anti-biofilm action involves multiple complex mechanisms affecting cells adhesion, extracellular matrix production, the quorum sensing indole balance and bacterial motility also making biofilm more prone to be dethatched from the surface.[23,44-46] It has been speculated that both molecules exploit their anti-biofilm performances by a ROS-based mechanism that modulates the activity of some proteins resulting in a decrease of biofilm formation. Indeed, cells use ROS as a signal or cue to adapt to a changing environment.[47]

Recently, it has been found that *E. coli* proteins targeted by ZA[16] and SA[23] are widespread with a high percentage of identity in a wide range of microorganisms, included several *E. coli* pathogenic stains and bacteria involved in serious disease. Thus, it is possible that LDPE-CA

and LDPE-ZA could exert their activity also against other bacterial strains. This opens the promising perspective to successfully extend this technology to a wide range of applications, especially in those field where mixed-species biofilms are the dominant form, e.g. in clinical, environmental, industrial, and agricultural areas.[47]

Conclusions

In this work, the functionalization of low-density polethylene coupons with biocide-free antibiofilm compounds was carried out to obtain new materials able to hinder biofilm formation. A low-pressure plasma reactor system was used for an efficient activation of the polymeric surfaces, as well as for the grafting-polymerization process. Several analytical techniques used to characterize each step of the functionalization process were described, and the obtained data were reported. As for the anti-biofilm evaluation, results showed that the process of graft-polymerization of the polyethylene did not affect *E. coli* sessile growth, while the grafting with *p*-aminosalicylic and *p*-aminocinnamic acids led to a significant decrease of biofilm biomass. In conclusion, two new materials with anti-adhesion properties were obtained by covalent linkage of molecules able to discourage biofilm formation without killing cells. Although the significant decrease in biomass is not guaranty of complete eradication of biofilm, the functionalized polymer might represent a step forward in short-term applications where it is required to slow down the contamination of the material. In many industrial and clinical activities, surface treatments able to retard adhesion, and consequently biofilm formation, could greatly enhance the efficiency of daily cleaning and disinfection procedures, because free-floating microbes are more sensitive to detergents and biocides then those in biofilms. Thus, the novel anti-biofilm materials can potentially extend the efficacy of the current arsenal of antimicrobial agents, and the functionalized polymers should be seen as integrated approaches to traditional control measures.

Acknowledgements

The authors acknowledge the financial support of the Fondazione Cariplo under Grant number 2011−0277.

The authors thank Dr. E. Pini, Dr. M.C. Sala, Dr. M. Cerea and Dr. C. Gennari (Department of Pharmaceutical Sciences) for analytical support and helpful discussions.

References

1. Cappitelli F, Sorlini C. Microorganisms attack synthetic polymers in items representing our cultural heritage", Applied and Environmental Microbiology 2008; 74(3): 564-569.
2. Armentano I, Arciola CR, Fortunati E, Ferrari D, Mattioli S, Amoroso CF, Rizzo J, Kenny JM, Imbriani M, Visai L. The interaction of bacteria with engineered nanostructured polymeric materials: a review 2014; Scientific World Journal 410423. doi: 10.1155/2014/410423.
3. Costerton JW. Introduction to biofilm. International Journal of Antimicrobial Agents 1999; 11:217-221.
4. Karatan E, Watnick P. Signals, Regulatory Networks, and Materials That Build and Break Bacterial Biofilms. Microbiology and Molecular Biology Reviews 2009; 73:310–347.
5. Cappitelli F, Principi P, Sorlini C. Biodeterioration of modern materials in Contemporary collections: can biotechnology help? Trends in Biotechnology 2006; 24(8): 350-354.
6. Davies D. Understanding biofilm resistance to antibacterial agents. Nat. Rev. Drug discovery 2003; 2:114-122.

7. Andersson D I, Hughes D, Antibiotic resistance and its cost: is it possible to reverse resistance? Nat Rev Microbiol 2010; 8:260-271.
8. Charnley M, Textor M, Acikgoz C. Designed polymer structures with antifouling-antimicrobial properties. Reactive & Functional Polymers 2011; 71:329-334.
9. Yoshimoto K, Nishio M, Sugasawa H, Nagasaki Y. Direct observation of adsorption-induced inactivation of antibody fragments surrounded by mixed-PEG layer on a gold surface. J Am Chem Soc 2010; 132:7982-7989.
10. Barrios CA, Xu Q, Cutright T, Newby BZ, Incorporating zosteric acid into silicone coatings to achieve its slow release while reducing fresh water bacterial attachment. Colloids Surf B 2005; 41:83-93.
11. Lu G, Wu D, Fu R. Studies on the synthesis and antibacterial activities of polymeric quaternary ammonium salts from dimethylaminoethyl methacrylate. Reactive and Functional Polymers 2007; 67:355-366.
12. Goddard JM, Hotchkiss JH. Polymer surface modification for the attachment of bioactive compounds. Progress in Polymer Science. 2007; 32: 698-725.
13. Darouiche RO. Prevention of infections associated with vascular catheters. Int J Artif Organs 2008; 31:810-819.
14. Wright GD Sutherland AD. New strategies for combating multidrug-resistant bacteria. Trends Mol Med 2007; 13:260-267.
15. Villa F, Villa S, Gelain A, Cappitelli F. Sub-lethal activity of small molecules from natural sources and their synthetic derivatives against biofilm forming Nosocomial pathogens. Curr Topics Med Chem 2013; 13: 3184-3204.
16. Cattò C, Dell'Orto S, Villa F, Villa S, Gelain A, Vitali A, Marzano V, Forlani F, Cappitelli F. Unravelling the Structural and Molecular Basis Responsible for the Anti-Biofilm Activity of Zosteric Acid PLoS ONE 2015; 10: e0136124.

17. Villa F, Albanese D, Giussani B, Stewart P, Daffonchio D. Cappitelli F. Hindering biofilm formation with zosteric acid. Biofouling 2010; 26:739-752.

18. Villa F, Pitts B, Stewart PS, Giussani B, Roncoroni S, Albanese D, Giordano C, Tunesi M, Cappitelli F. Efficacy of zosteric acid sodium salt on the yeast biofilm model Candida albicans. Microbial Ecol 2011; 62: 584-598.

19. Polo A, Foladori P, Ponti B, Bettinetti R, Gambino M, Villa F, Cappitelli F. Evaluation of zosteric acid for mitigating biofilm formation of Pseudomonas putida isolated from a membrane bioreactor system. Int J Mol Sci 2014; 15: 9497-9518.

20. Geiger T, Delavy P, Hany R, Schleuniger J, Zinn M. Encapsulated zosteric acid embedded in poly[3-hydroxyalkanoate] coatings-protection against biofouling. Polym. Bul. 2004; 52: 65-72.

21. Rasko D A, Sperandio V. Anti-virulence strategies to combat bacteria-mediated disease. Nature Reviews Drug Discovery 2010; 9:117-128.

22. Francolini I, Donelli G. Prevention and control of biofilm-based medical-device-related infections. FEMS Immunology and Medical Microbiology 2010; 59: 227-238.

23. Cattò C, Grazioso G, Dell'Orto S, Gelain A, Villa S, Marzano V, Vitali A, Villa F, Cappitelli, F, Forlani F, The response of Escherichia coli biofilm to salicylic acid. Biofouling 2017; DOI:10.1080/08927014.2017.1286649

24. Lieberman MA, Lichtenberg AJ Principles of Plasma Discharges and Materials Processing, New York: Wiley; 1994.

25. Lai B, Sunderland J, Xue S, Yan W, Zhao M, Folkard M, Michael BD, Wang Y, Study on hydrophilicity of polymer surfaces improved by plasma treatment. Appl Surf Sci 2006; 252: 3375-3379.

26. Vassallo E, Cremona A, Ghezzi F, Ricci D. Characterization by optical emission spectroscopy of an oxygen plasma used for improving PET wettability Vacuum 2010; 84: 902-906.

27. Zanini S, Riccardi C, Orlandi M, Colombo C, Croccolo F. Plasma-induced graft-polymerisation of ethylene glycol methacrylate phosphate on polyethylene films. Polymer Degradation and Stability 2008; 93: 1158-1163.

28. Corbin A, Pitts B, Parker A, Stewart PS. Antimicrobial Penetration and Efficacy in an In vitro Oral Biofilm Model. Antimicrobial Agents and chemotherapy. 2011; 55:3338-3344.

29. Faucher SP, Charette SJ. Editorial on: Bacterial pathogens in the non-clinical environment. Front Microbiol 2011; 6:331.

30. Hayashi K, Morooka N, Yamamoto Y, Fujita K, Isono K, Choi S, Ohtsubo E, Baba T, Wanner BL, Mori H, Horiuchi T. Highly accurate genome sequences of Escherichia coli K-12 strains MG1655 and W3110. Mol Syst Biol 2006; 2:2006.0007.

31. Kim W, Choi H S, Surface crosslinking of high-density polyethylene beads in a modified plasma reactor J Appl Polym Sci, 2002; 83: 2921-2929.

32. Sommerfeld Ross S, Tu MH, Falsetta ML, Ketterer MR, Kiedrowski MR, Horswill AR, Apicella MA, Reinhardt JM, Fiegel J. Quantification of confocal images of biofilms grown on irregular surfaces. J Microbiol Methods 2014; 100:111-120.

33. Villa F, Remelli W, Forlani F, Gambino M, Landini P, Francesca Cappitelli F. Effects of chronic sub-lethal oxidative stress on biofilm formation by Azotobacter vinelandii , Biofouling: The Journal of Bioadhesion and Biofilm Research 2012; 28:8, 823-833.

34. Heydorn A, Nielsen AT, Hentzer M, Sternberg C, Givskov M, Kjær Ersbøll B, Molin S. Quantification of biofilm structures by the novel computer program COMSTAT. 2000; Microbiology 146: 2395-2407.

35. de Carvalho CCCR, da Fonseca MR. 2007. Assessment of three-dimensional biofilm structure using an optical microscope. BioTechniques 2007; 42: 616-620.

36. Kim W, Choi HS, Surface crosslinking of high-density polyethylene beads in a modified plasma reactor J Appl Polym Sci 2002; 83: 2921-2929.

37. Sanchis MR, Blanes V, Blanes M, Garcia D, Balart R. Surface modification of low density polyethylene (LDPE) film by low pressure O2 plasma treatment. European Polymer Journal 2006; 42: 1558–1568.

38. Lehocký M, Drnovská H, Lapčíková B, Barros-Timmons A M, Trindade T, Zembala M, Lapčík, L. Plasma surface modification of polyethylene. Colloids and Surfaces A: Physicochemical and Engineering Aspects. 2003; 222: 125-131.

39. Suyal K, Joshi N K, Rautela R, Joshi HC, Pant S. Fluorescence properties of 4-amino salicylic acid in polymers. Journal of Photochemistry and Photobiology A: Chemistry. 2010; 216: 51-58.

40. Farber BF, Wolff AG. Salicylic acid prevents the adherence of bacteria and yeast to silastic catheters. J Biomed Mater Res 1993; 27:599–602.

41. Xu Q., Barrios C.A., Cutright T., Newby B.Z. Evaluation of toxicity of capsaicin and zosteric acid and their potential application as antifoulants. Environmental Toxicology 2005; 20: 467-474.

42. Rudrappa T, Quinn WJ, Stanley-Wall NR, Bais HP. A degradation product of the salicylic acid pathway triggers oxidative stress resulting in down-regulation of *Bacillus subtilis* biofilm formation on Arabidopsis thaliana roots. Planta 2007; 226:283–297.

43. Villa F, Remelli W, Forlani F, Vitali A, Cappitelli F. Altered expression level of *Escherichia coli* proteins in response to treatment with the antifouling agent zosteric acid sodium salt. Environ Microbiol 2012; 14:1753–1761.

44. Vila J, Soto SM. Salicylate increases the expression of marA and reduces *in vitro* biofilm formation in uropathogenic *Escherichia coli* by decreasing type 1 fimbriae expression. Virulence 2012; 3:280–285.

45. Dong Y, Huang C, Park J, Wang G. Growth Inhibitory Levels of Salicylic Acid Decrease Pseudomonas aeruginosa fliC Flagellin Gene Expression Journal of Experimental Microbiology and Immunology 2012; 16:73-78.

46. Cap M, Váchová L, Palková Z. Reactive oxygen species in the signaling and adaptation of multicellular microbial communities. Oxidative Medicine and Cellular Longevity 2012; doi:10.1155/2012/976753.

47. Sivan E, Ehud B. Multi-species biofilms: living with friendly neighbors FEMS Microbiol. Rev 2012;36:990–1004.

Figures legend

Figure 1 Schematic diagram illustrating the graft copolymerization of HEMA into the plasma pretreated LDPE surface.

Figure 2 SEM images of coupons subjected to different treatments. A) clean LDPE; B) LDPE after plasma reactor treatment.

Figure 3 XPS wide scan spectra of oxygen plasma activated low density polyethylene (Panel a), low density polyethylene functionalized with *p*-aminocinnamic acid (LDPE-CA) (Panel b) and low density polyethylene functionalized with *p*-aminosalicylic acid (LDPE-SA) (Panel c).

Figure 4 ATR-FTIR spectra of treated (b,c) and untreated samples (a). The typical peaks of the amide bond confirmed the presence of a covalent bond between *p*-aminosalicylic acid (b) and *p*- aminocinnamic acid (c) after graft-polymerization to the supporting material (a).

Figure 5 Fluorescence spectroscopy analysis of polyethylene functionalization with *p*-aminosalicylic acid and *p*-aminocinnamic acid. Emission spectra of free *p*-aminosalicylic (λ_{exc}

= 325 nm) and *p*-aminocinnamic acids (λ_{exc} = 380 nm) in 0.4 M $NaHCO_3$, 1 M NaCl (pH 8.3) are reported in panel a and b, respectively. The solid surface fluorescence emission spectra of coupons functionalized with *p*-aminosalicylic (λ_{exc} = 334 nm) and *p*-aminocinnamic acids (λ_{exc} = 385 nm) are reported in panel c and d, respectively. In c and d, replicated surface fluorescence emission spectra of the functionalized coupons were cumulated, and displayed after subtraction by cumulated surface fluorescence emission of the untreated (LDPE-HEMA-COOH) coupons. A. U., arbitrary units

Figure 6 Representative CLSM images of control and functionalized coupons, before and after consecutively growing biofilm for 10 times on their surface by CDC reactor. Blue fluorescence corresponds to the molecule presence on the surface. First line (before growing biofilm): a) LDPE-HEMA-COOH-DCC; b) LDPE-SA; c) LDPE-CA. Second line (after growing biofilm): d) LDPE-SA; e) LDPE-CA. Scale bar = 40 µm.

Figure 7 Representative epifluorescence microscope images of intact (a-c) and cryosectioned (d-f) *E. coli* biofilm stained with CellMask plasma membrane orange and grown on functionalized and non-functionalized polyethylene surfaces (60x, 1.0 NA water immersion objective). a, d) LDPE;b, e) LDPE-CA; c, f) LDPE-SA. Red fluorescence corresponds to *E. coli* cells. λex: 554 nm and λem: 567. Scale bar = 30 µm. g: Surface coverage, thickness and cell biovolume of *E. coli* biofilm grown on functionalized and non-functionalized coupons. Data represent the mean ± standard deviation of three independent experiments. Different superscript letters indicate significant differences (Tukey's HSD, $p \leq 0.05$) between the means of different surfaces.

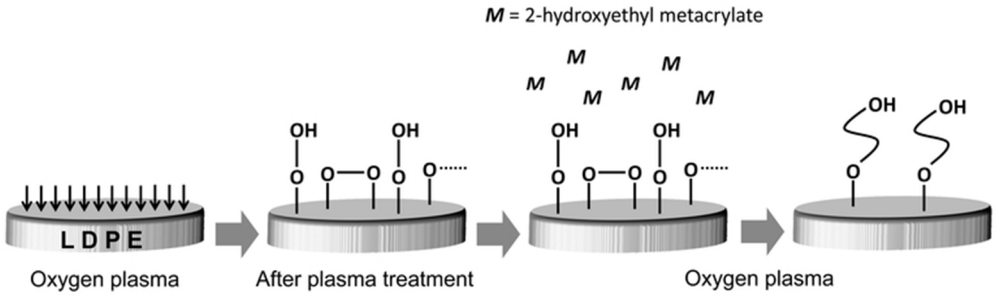

Figure 1 Schematic diagram illustrating the graft copolymerization of HEMA into the plasma pretreated LDPE surface.

32x10mm (600 x 600 DPI)

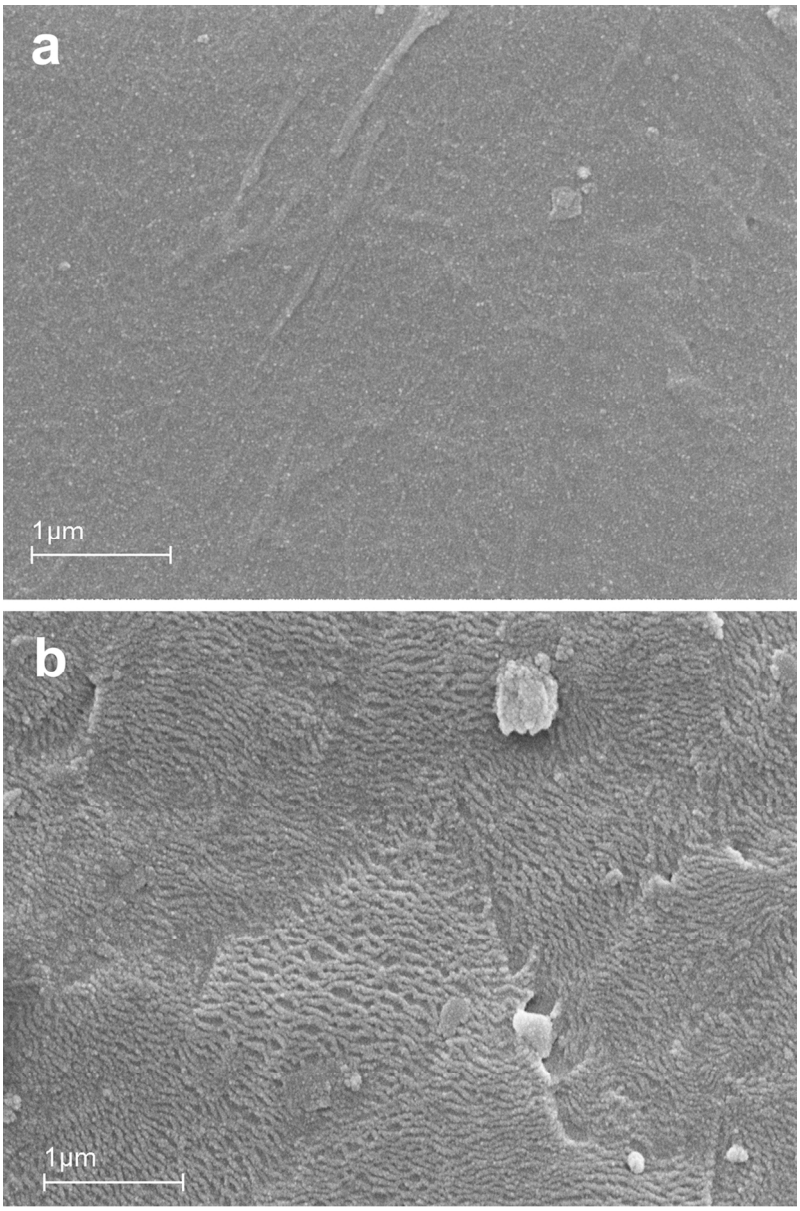

Figure 2 SEM images of coupons subjected to different treatments. A) clean LDPE; B) LDPE after plasma reactor treatment.

101x153mm (300 x 300 DPI)

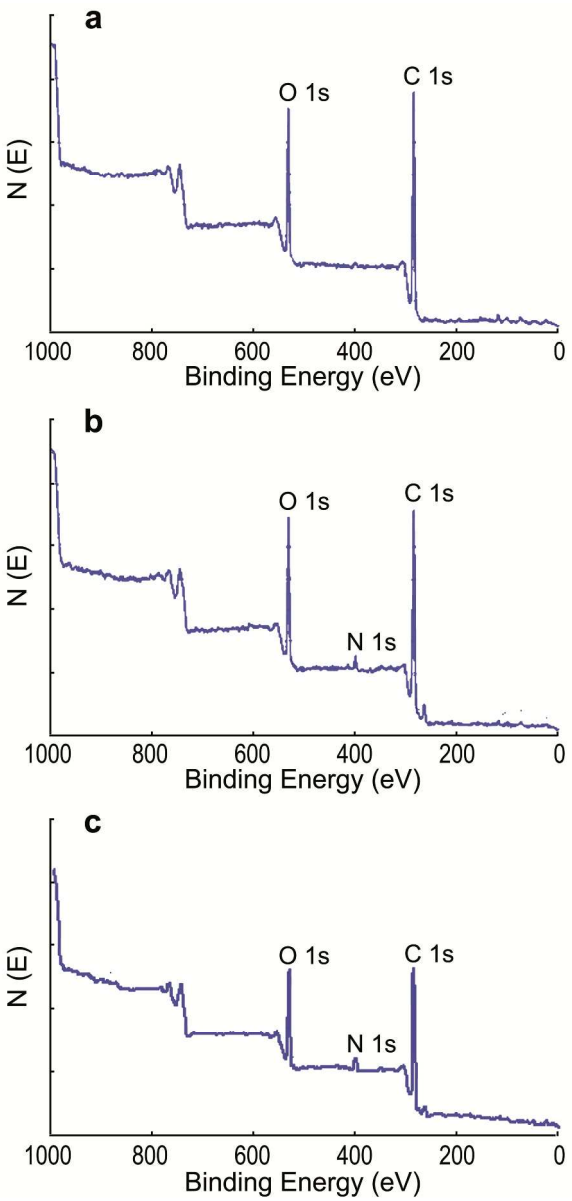

Figure 3 XPS wide scan spectra of oxygen plasma activated low density polyethylene (Panel a), low density polyethylene functionalized with *p*-aminocinnamic acid (LDPE-CA) (Panel b) and low density polyethylene functionalized with *p*-aminosalicylic acid (LDPE-SA) (Panel c).

101x210mm (600 x 600 DPI)

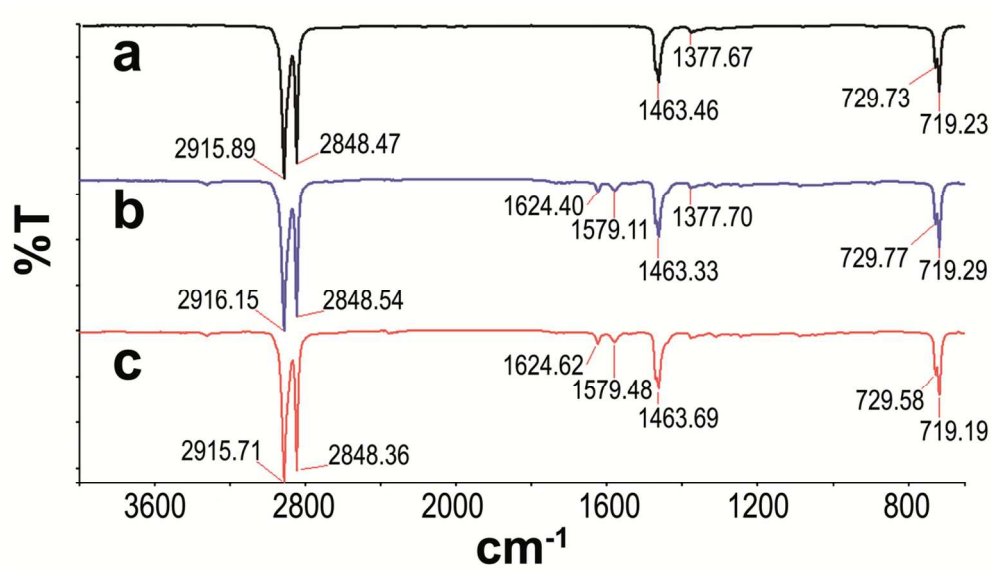

Figure 4 ATR-FTIR spectra of treated (b,c) and untreated samples (a). The typical peaks of the amide bond confirmed the presence of a covalent bond between p-aminosalicylic acid (b) and p- aminocinnamic acid (c) after graft-polymerization to the supporting material (a).

58x33mm (600 x 600 DPI)

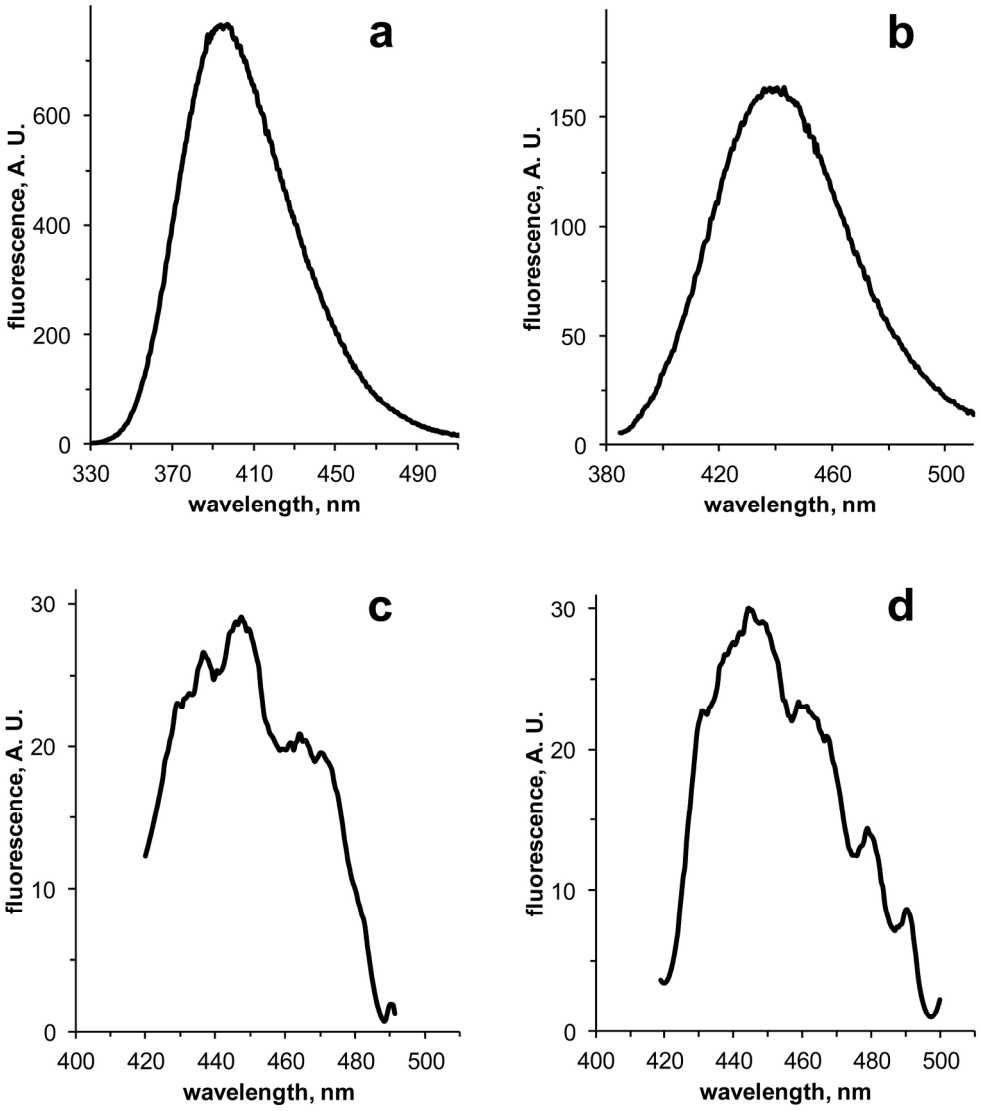

Figure 5 Fluorescence spectroscopy analysis of polyethylene functionalization with *p*-aminosalicylic acid and *p*-aminocinnamic acid. Emission spectra of free *p*-aminosalicylic (λexc = 325 nm) and *p*-aminocinnamic acids (λexc = 380 nm) in 0.4 M $NaHCO_3$, 1 M NaCl (pH 8.3) are reported in panel a and b, respectively. The solid surface fluorescence emission spectra of coupons functionalized with *p*-aminosalicylic (λexc = 334 nm) and *p*-aminocinnamic acids (λexc = 385 nm) are reported in panel c and d, respectively. In c and d, replicated surface fluorescence emission spectra of the functionalized coupons were cumulated, and displayed after subtraction by cumulated surface fluorescence emission of the untreated (LDPE-HEMA-COOH) coupons. A. U., arbitrary units

101x113mm (600 x 600 DPI)

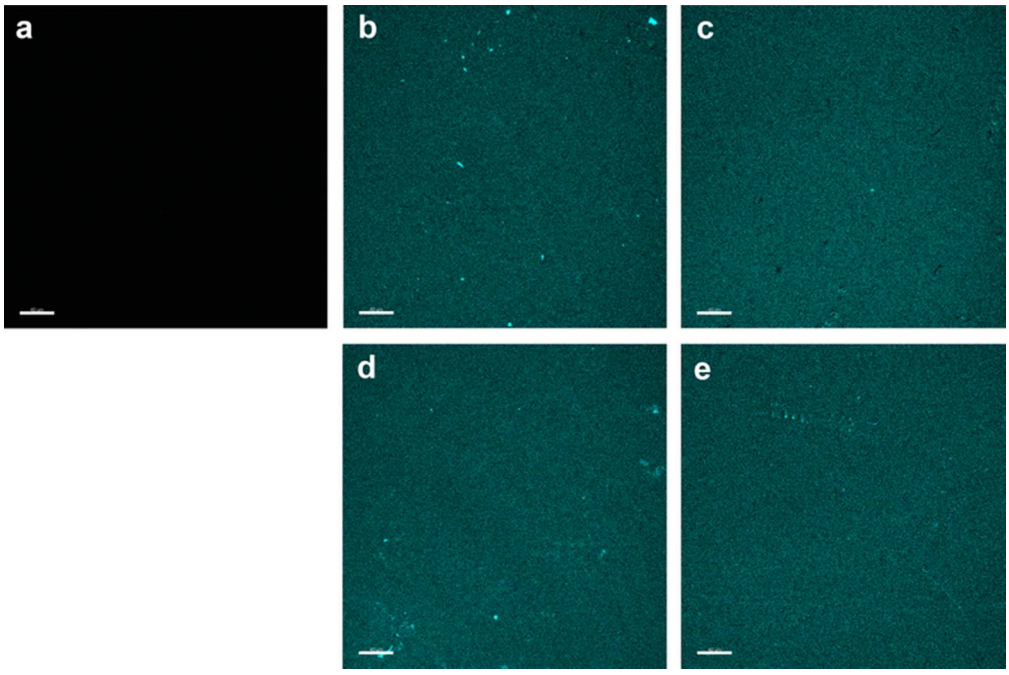

Figure 6 Representative CLSM images of control and functionalized coupons, before and after consecutively growing biofilm for 10 times on their surface by CDC reactor. Blue fluorescence corresponds to the molecule presence on the surface. First line (before growing biofilm): a) LDPE-HEMA-COOH-DCC; b) LDPE-SA; c) LDPE-CA. Second line (after growing biofilm): d) LDPE-SA; e) LDPE-CA. Scale bar = 40 μm.

67x44mm (300 x 300 DPI)

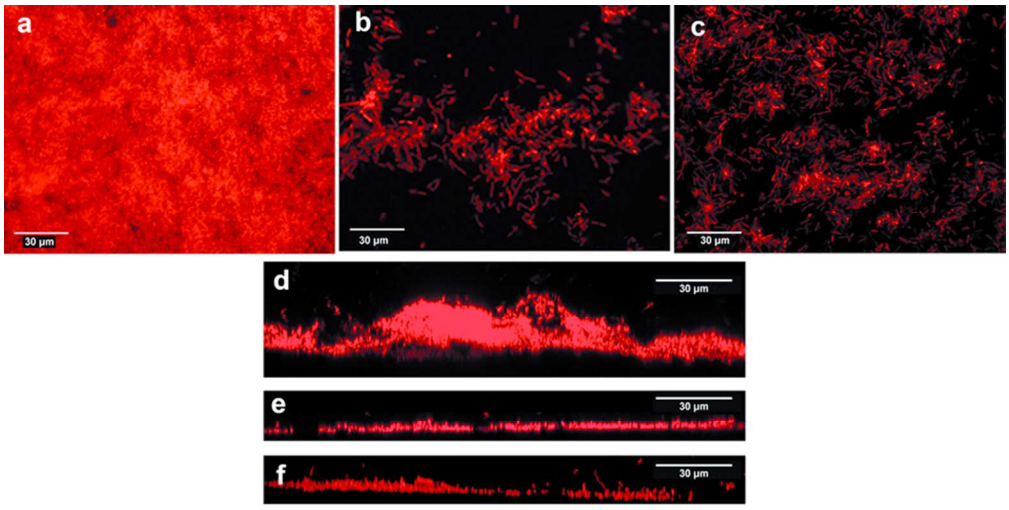

g

	Surface coverage (%)	Mean thickness (µm)	Cell volume (× 10^5 µm³)*
LDPE	91.0±3.9 [a]	20.5±3.9 [a]	7.22±1.40 [a]
LDPE-OH	87.4±3.7 [a]	18.9±2.7 [a]	6.39±0.95 [a]
LDPE-COOH	92.8±1.0 [a]	19.2±3.8 [a]	6.89±1.37 [a]
LDPE-CA	24.0±6.1 [b]	3.1±0.8 [b]	0.29±0.11 [b]
LDPE-SA	33.3±3.8 [b]	5.1±1.0 [b]	0.66±0.15 [b]

*data referred to the same surface area

Figure 7 Representative epifluorescence microscope images of intact (a-c) and cryosectioned (d-f) *E. coli* biofilm stained with CellMask plasma membrane orange and grown on functionalized and non-functionalized polyethylene surfaces (60x, 1.0 NA water immersion objective). a, d) LDPE;b, e) LDPE-CA; c, f) LDPE-SA. Red fluorescence corresponds to *E. coli* cells. λex: 554 nm and λem: 567. Scale bar = 30 µm. g: Surface coverage, thickness and cell biovolume of E. coli biofilm grown on functionalized and non-functionalized coupons. Data represent the mean ± standard deviation of three independent experiments. Different superscript letters indicate significant differences (Tukey's HSD, $p \leq 0.05$) between the means of different surfaces.

73x53mm (300 x 300 DPI)